A source of 2 terawatt, 2.7 cycle laser pulses based on noncollinear optical parametric chirped pulse amplification

S. Witte, R. Th. Zinkstok, A. L. Wolf, W. Hogervorst, W. Ubachs and K. S. E. Eikema

Atomic, Molecular, and Laser Physics Group, Laser Centre Vrije Universiteit, De Boelelaan 1081, 1081 HV Amsterdam, The Netherlands

kse.eikema@few.vu.nl

Abstract: We demonstrate a noncollinear optical parametric chirped pulse amplifier system that produces 7.6 fs pulses with a peak power of 2 terawatt at 30 Hz repetition rate. Using an ultra-broadband Ti:Sapphire seed oscillator and grating-based stretching and compression combined with an LCD phase-shaper, we amplify a 310 nm wide spectrum with a total gain of 3×10^7, and compress it within 5% of its Fourier limit. The total integrated parametric fluorescence is kept below 0.2%, leading to a pre-pulse contrast of 2×10^{-8} on picosecond timescales.

OCIS codes: (140.3280) Laser amplifiers; (190.4970) Parametric oscillators and amplifiers; (320.7090) Ultrafast lasers; (320.7160) Ultrafast technology

References and links

1. T. Brabec and F. Krausz, "Intense few-cycle laser fields: Frontiers of nonlinear optics," Rev. Mod. Phys. **72**, 545-591 (2000).
2. A. Scrinzi, M. Yu. Ivanov, R. Kienberger, and D. M. Villeneuve, "Attosecond physics," J. Phys. B **39**, R1-R37 (2006).
3. H. Niikura, D. M. Villeneuve, and P. B. Corkum, "Controlling vibrational wave packets with intense, few-cycle laser pulses," Phys. Rev. A **73**, 021402(R) (2006).
4. A. Dubietis, G. Jonušauskas, and A. Piskarskas, "Powerful femtosecond pulse generation by chirped and stretched pulse parametric amplification in BBO crystal," Opt. Commun. **88**, 437-440 (1992).
5. I. N. Ross, P. Matousek, M. Towrie, A. J. Langley, and J. L. Collier, "The prospects for ultrashort pulse duration and ultrahigh intensity using optical parametric chirped pulse amplification," Opt. Commun. **144**, 125-133 (1997).
6. I. N. Ross, J. L. Collier, P. Matousek, C. N. Danson, D. Neely, R. M. Allott, D. A. Pepler, C. Hernandez-Gomez, and K. Osvay, "Generation of terawatt pulses by use of optical parametric chirped pulse amplification," Appl. Opt. **39**, 2422-2427 (2000).
7. V. V. Lozhkarev, G. I. Freidman, V. N. Ginzburg, E. V. Katin, E. A. Khazanov, A. V. Kirsanov, G. A. Luchinin, A. N. Mal'shakov, M. A. Martyanov, O. V. Palashov, A. K. Poteomkin, A. M. Sergeev, A. A. Shaykin, I. V. Yakovlev, S. G. Garanin, S. A. Sukharev, N. N. Rukavishnikov, A. V. Charukhchev, R. R. Gerke, and V. E. Yashin, "200 TW 45 fs laser based on optical parametric chirped pulse amplification," Opt. Express 14, 446-454 (2006)
8. R. Th. Zinkstok, S. Witte, W. Hogervorst, and K. S. E. Eikema, "High-power parametric amplification of 11.8-fs laser pulses with carrier-envelope phase control," Opt. Lett. **30**, 78-80 (2005).
9. S. Witte, R. Th. Zinkstok, W. Hogervorst, and K. S. E. Eikema, "Generation of few-cycle terawatt light pulses using optical parametric chirped pulse amplification," Opt. Express **13**, 4903-4908 (2005).
10. N. Ishii, L. Turi, V. S. Yakovlev, T. Fuji, F. Krausz, A. Baltuška, R. Butkus, G. Veitas, V. Smilgevicius, R. Danielius, and A. Piskarskas, "Multimillijoule chirped parametric amplification of few-cycle pulses," Opt. Lett. **30**, 567-569 (2005).
11. T. Fuji, N. Ishii, C. Y. Teisset, X. Gu, Th. Metzger, A. Baltuška, N. Forget, D. Kaplan, A. Galvanauskas, and F. Krausz, "Parametric amplification of few-cycle carrier-envelope phase-stable pulses at 2.1 μm," Opt. Lett. **31**, 1103-1105 (2006).

#72557 - $15.00 USD Received 30 June 2006; revised 18 August 2006; accepted 25 August 2006

12. D. Kraemer, R. Hua, M. L. Cowan, K. Franjic, and R. J. D. Miller, "Ultrafast noncollinear optical parametric chirped pulse amplification in $KTiOAsO_4$," Opt. Lett. **31**, 981-983 (2006).
13. I. N. Ross, P. Matousek, G. H. C. New, and K. Osvay, "Analysis and optimization of optical parametric chirped pulse amplification," J. Opt. Soc. Am. B **19**, 2945-2956 (2002).
14. X. Yang, Z. Xu, Z. Zhang, Y. Leng, J. Peng, J. Wang, S. Jin, W. Zhang, and R. Li, "Dependence of spectrum on pump-signal angle in BBO-I noncollinear optical-parametric chirped-pulse amplification," Appl. Phys. B **73**, 219-222 (2001).
15. A. J. Verhoef, J. Seres, K. Schmid, Y. Nomura, G. Tempea, L. Veisz, and F. Krausz, "Compression of the pulses of a Ti:Sapphire laser system to 5 femtoseconds at 0.2 terawatt level," Appl. Phys. B **82**, 513-517 (2006).
16. J. H. Sung, J. Y. Park, T. Imran, Y. S. Lee, C. H. Nam, "Generation of 0.2-TW 5.5-fs optical pulses at 1 kHz using a differentially pumped hollow-fiber chirped-mirror compressor," Appl. Phys. B **82**, 5-8 (2006).
17. G. Stibenz, N. Zhavoronkov, and G. Steinmeyer, "Self-compression of millijoule pulses to 7.8 fs duration in a white-light filament," Opt. Lett. **31**, 274-276 (2006).
18. H. Takada and K. Torizuka, "Design and construction of a TW-class 12-fs Ti:Sapphire chirped-pulse amplification system," IEEE J. Sel. Top. Quantum Electron. **12**, 201-212 (2006).
19. C. Iaconis and I. A. Walmsley, "Spectral phase interferometry for direct electric-field reconstruction of ultrashort optical pulses," Opt. Lett. **23**, 792-794 (1998).
20. E. J. Divall and I. N. Ross, "High dynamic range contrast measurements by use of an optical parametric amplifier correlator," Opt. Lett. **29**, 2273-2275 (2004).
21. F. Tavella, K. Schmid, N. Ishii, A. Marcinkevičius, L. Veisz and F. Krausz, "High-dynamic range pulse-contrast measurements of a broadband optical parametric chirped-pulse amplifier," Appl. Phys. B **81**, 753-756 (2005).
22. K. Osvay, M. Csatári, I. N. Ross, A. Persson, and C.-G. Wahlström, "On the temporal contrast of high intensity femtosecond laser pulses," Laser Part. Beams **23**, 327-332 (2005).
23. J. C. Vaughan, T. Feurer, K. W. Stone, and K. A. Nelson, "Analysis of replica pulses in femtosecond pulse shaping with pixelated devices," Opt. Express **14**, 1314-1328 (2006).

1. Introduction

The generation of high-intensity few-cycle laser pulses is a subject of great interest [1], as experimental progress in fields such as attosecond science [2] and quantum control [3] is for a large part dependent on the availability of suitable laser sources. In recent years, optical parametric chirped pulse amplification (OPCPA) [4, 5] has been demonstrated to be a very promising technique for the production of ultrashort, high-intensity laser pulses [6, 7]. Especially the development of OPCPA in a noncollinear geometry (NOPCPA) has facilitated the amplification of ultra-broadband spectra both in the Ti:Sapphire wavelength range [8, 9, 10] and at longer wavelengths [11, 12].

In this paper we present an NOPCPA system that produces 2 terawatt peak intensity laser pulses with a duration of 2.7 optical cycles (7.6 fs). The system utilizes the full $>$300 nm gain bandwidth that has been theoretically predicted for a 532 nm pumped NOPCPA system [13, 14] based on BBO (β-barium borate) crystals, while maintaining spectral phase control over this entire bandwidth. State-of-the-art few-cycle laser sources can deliver sub-3-cycle pulses with an intensity reaching 0.2 TW [15, 16, 17]; therefore, our system represents an order of magnitude increase in peak intensity in sub-3-cycle pulse generation, with excellent prospects for further power scaling.

2. Ultra-broadband two terawatt NOPCPA system

As parametric amplification is an instantaneous nonlinear optical process, efficient amplification can only be achieved by matching the duration of pump and seed pulses. In OPCPA, an ultrashort, broadband seed pulse is stretched to match its duration to a long, high-energy pump pulse from e.g. a Nd:YAG laser system. Energy transfer and subsequent recompression of the amplified seed pulse then leads to the production of ultrashort high-energy pulses. Specifically, a combination of BBO as the nonlinear medium, a pump wavelength around 532 nm, and a small noncollinear angle ($\sim$2.4°) leads to an extremely broad gain bandwidth in the near-infrared, potentially supporting the amplification of 7 fs pulses from a Ti:Sapphire laser [5]. An

#72557 - $15.00 USD Received 30 June 2006; revised 18 August 2006; accepted 25 August 2006

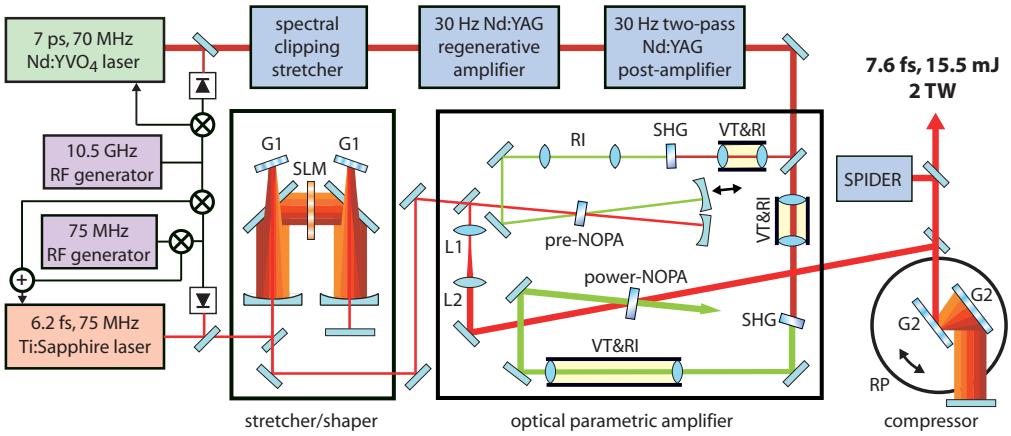

Fig. 1. Schematic of the 2 TW, 7.6 fs NOPCPA system. G1: 600 l/mm grating, G2: 1200 l/mm grating, SLM: 640-element LCD spatial light modulator, VT: vacuum tube, RI: relay-imaging, RP: rotatable platform, SHG: crystal for second harmonic generation. The lenses L1 and L2 are drawn for simplicity, in practice only reflective optics are used in the seed beam path. See text for further details.

additional advantage of optical parametric amplification is that the single-pass gain can exceed 10^3, allowing large amplification factors to be achieved in a very compact setup.

We have designed a laser amplifier system that exploits these benefits of NOPCPA to generate terawatt-level few-cycle pulses. Key elements of this system are: 1) A compact, three-pass amplifier with a gain of 3×10^7; 2) A stretcher-compressor combination capable of accurate spectral phase compensation over a $>$300 nm bandwidth; 3) A pump pulse duration in the 10-100 ps range and hence a moderate stretching ratio ($\sim10^3$); 4) Pump-seed synchronization with sub-picosecond accuracy. All these features are implemented in the setup shown in Fig. 1.

The seed laser is a home-built ultra-broadband Ti:Sapphire oscillator, which produces 5.5 nJ pulses at 75 MHz repetition rate, with a spectrum that has a Fourier-limit of 6.2 fs. All cavity mirrors have a broadband multilayer coating (Layertec) with negative GVD ranging from -50 to -70 fs^2. In combination with the dispersion due to a 1 mm fused silica plate, two thin fused silica wedges and the 2.5 mm optical path length Ti:Sapphire crystal, this yields compensation of the dispersion from roughly 670 to 950 nm. The repetition rate of this oscillator is locked to the signal of a 75 MHz RF generator using a piezo-mounted mirror in the laser cavity. For increased stability, we employ an additional lock at the 140th harmonic (10.5 GHz) of the repetition rate, which is generated in a fast photodiode. The seed pulses are stretched to about 13 ps using a grating-based pulse stretcher, in which a 640-element LCD phase-only spatial light modulator (Jenoptik) is incorporated for high-resolution spectral phase control. From the available seed light, 4 nJ pulses are sent into the stretcher, which has a transmission of 25%. A more detailed discussion of pulse stretching and compression is given in section 3.

The pump laser source is based on amplification of pulses from a SESAM modelocked 70 MHz Nd:YVO_4 oscillator (High-Q Laser). This laser is synchronized to the Ti:Sapphire oscillator by locking the 150th harmonic of its repetition frequency to the same 10.5 GHz RF generator that is used for the Ti:Sapphire laser stabilization. Such a locking scheme ensures that every 14th pulse from the Nd:YVO_4 laser (corresponding to a 200 ns delay) overlaps with every 15th Ti:Sapphire laser pulse. At the lower repetition rate of an amplifier system (30 Hz in the present case) this then leads to properly synchronized pulses, provided the amplifier pulse repetition period is an integer multiple of the aforementioned 200 ns time delay.

#72557 - $15.00 USD Received 30 June 2006; revised 18 August 2006; accepted 25 August 2006

The pulses from the Nd:YVO_4 oscillator are first stretched to 60 ps in time to allow amplification to higher energy without damaging optics. This is done by dispersing the spectrum of the pulses in a $4f$-setup and cutting away a large part of the spectrum with a slit in the Fourier plane. The 60 ps pulses are then amplified to the mJ level in a diode-pumped Nd:YAG regenerative amplifier. The regenerative amplifier causes some reshaping of the pump pulse, as it operates at a power level where the effects of self-phase-modulation and self-compression start to become appreciable. To limit the influence of these effects the regenerative amplifier is not operated at full saturation. From an autocorrelation measurement, we confirmed that the pump pulse has a smooth shape without significant pre- or postpulses. Further amplification up to 250 mJ per pulse at 30 Hz repetition rate is achieved with a double-pass post-amplifier containing two flashlamp-pumped Nd:YAG modules (EKSPLA Ltd.) in a ring geometry. After second harmonic generation (SHG), up to 160 mJ per pulse is produced at 532 nm. This pump laser system will be explained in detail in a future paper. The difference in pulse duration between pump and seed (60 ps vs. 13 ps) is chosen such that the pump intensity variation is relatively small across the entire chirped seed pulse. Consequently, all spectral components in the seed pulse experience similar gain, which improves the width of the amplified spectrum. As the wings of the seed spectrum extend considerably beyond the 13 ps FWHM duration of the stretched seed pulse, saturation in the last pass still ensures a good energy extraction efficiency [9].

The actual NOPCPA system consists of only three amplification passes: two in a pre-amplifier pumped by 10 mJ 532 nm pulses, and a final pass through a power-amplifier crystal pumped by 150 mJ of pump light. The pre-amplifier contains a 5.5 mm long BBO crystal ($\theta = 22.5^\circ$, $\phi = 0^\circ$, type I phase matching) as the gain medium. Both pump and seed beam are collimated to a 1.5 mm diameter, and intersect with a noncollinear angle of about 2.4° inside the crystal. The noncollinear angles in the two passes through the pre-amplifier are aligned slightly differently to optimize the output spectral bandwidth. The pre-amplifier increases the energy of the seed pulses from 1 nJ to about 0.5 mJ.

After the pre-amplifier, the beam is expanded to 10 mm diameter by a telescope, and amplified to 30 mJ per pulse in a single pass through the power-amplifier stage. This power-amplifier has a 5 mm long, 14 mm × 14 mm BBO crystal (phase-matching angles identical to the pre-amplifier crystal) as the gain medium. Similar to the pre-amplifier, the noncollinear angle is near 2.4°, and optimized by maximizing the amplified bandwidth.

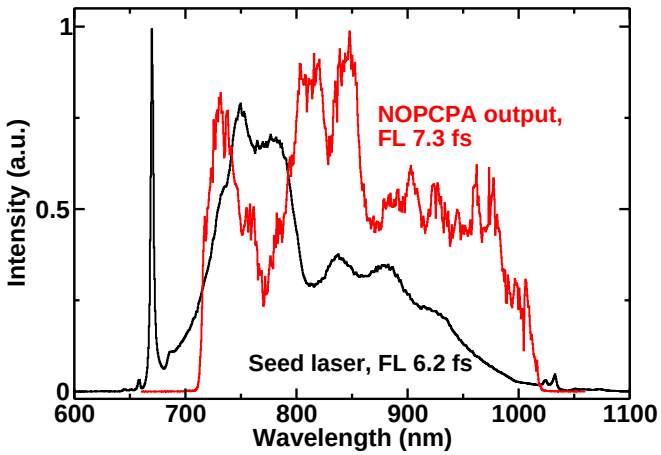

Fig. 2. The oscillator spectrum (black curve), and the NOPCPA output after amplification to 30 mJ per pulse and subsequent pulse compression (red curve). FL: Fourier limit.

#72557 - $15.00 USD Received 30 June 2006; revised 18 August 2006; accepted 25 August 2006

As the transverse beam profile of the pump laser has a top-hat distribution, relay-imaging is applied between the final Nd:YAG amplifier rod in the pump laser and the SHG crystals, as well as between the SHG crystals and the respective OPA amplifier stages. The relay-imaging ensures a good-quality pump beam profile in the OPA crystals. This is of paramount importance for proper NOPCPA operation as gain, pulse contrast and beam profile of the amplified seed beam are all strongly affected by the pump beam profile. Where needed, the focus that occurs in the Fourier plane of the relay-imaging systems has been placed in a vacuum tube to prevent optical breakdown and self-phase-modulation in air.

Fig. 2 displays a typical spectrum of the oscillator output, and one of the amplified and recompressed pulses after the full NOPCPA system. The part of the oscillator spectrum below 700 nm is actually not transmitted by the stretcher; as the phase mismatch of the parametric amplification process becomes too high for wavelengths below 710 nm to have any significant gain, the stretcher has been designed for spectra between 700 nm and 1100 nm. Fig. 2 clearly shows the rectangular spectral shape characteristic of a saturated NOPCPA, and the amplified spectrum extends from about 710 nm to 1020 nm. The width of the generated spectrum is very close to the theoretically predicted limit for an NOPCPA system based on 5 mm long BBO crystals and a pump wavelength of 532 nm [5, 13, 14]. The Fourier limit of the NOPCPA output is 7.3 fs FWHM, which corresponds to a 2.5 cycle pulse at a carrier wavelength of 850 nm. The intensity stability of the OPA output is measured to be 4% RMS, which is mainly the result of the 2.5% RMS fluctuations of the pump intensity.

While the initial beam profile of the Ti:Sapphire oscillator output is Gaussian, the beam profile of the amplified NOPCPA output adopts the top-hat shape of the pump laser due to saturation (Figs. 3(a) and 3(b)). To investigate the possibility of spatial chirp in the amplified beam, we measured the spectrum in various parts of the beam using a fiber-coupled spectrometer. Although some spectral variations across the beam have been observed, no systematic spatial chirp is detected. Additional information has been obtained by recording the beam profile with various interference filters in the beam (see Fig. 3(c)). These pictures show some variations, mostly in the regions of low spectral amplitude. This structure is attributed to the wavelength dependent phase-matching and sensitivity to perturbations in the pump beam wavefront, leading to some differences in gain and saturation.

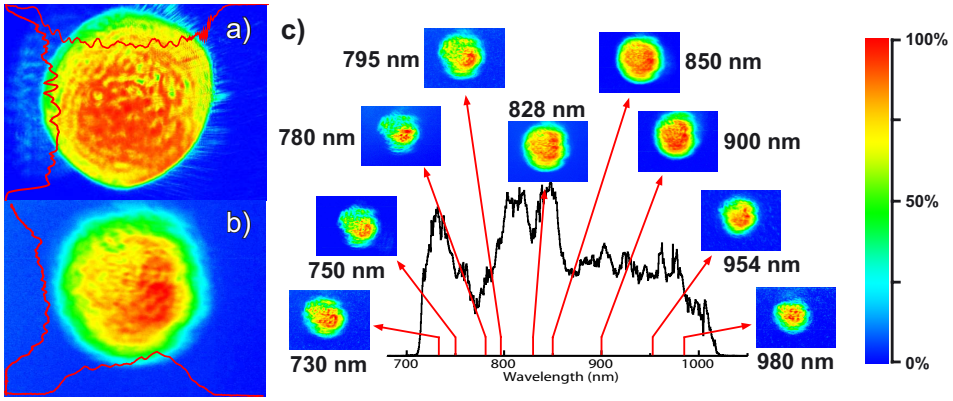

Fig. 3. (a) Beam profile of the pump laser in the power-amplifier stage. (b) Beam profile of the amplified OPA output beam in the power-amplifier stage. (c) Measured beam profile of the OPA output for various parts of the spectrum. All pictures were taken by relay-imaging the beam in the power-amplifier crystal onto a CCD camera. The red traces in (a) and (b) represent the beam profile across the center of the respective beams, averaged over 10 rows (or columns) of pixels.

#72557 - $15.00 USD Received 30 June 2006; revised 18 August 2006; accepted 25 August 2006

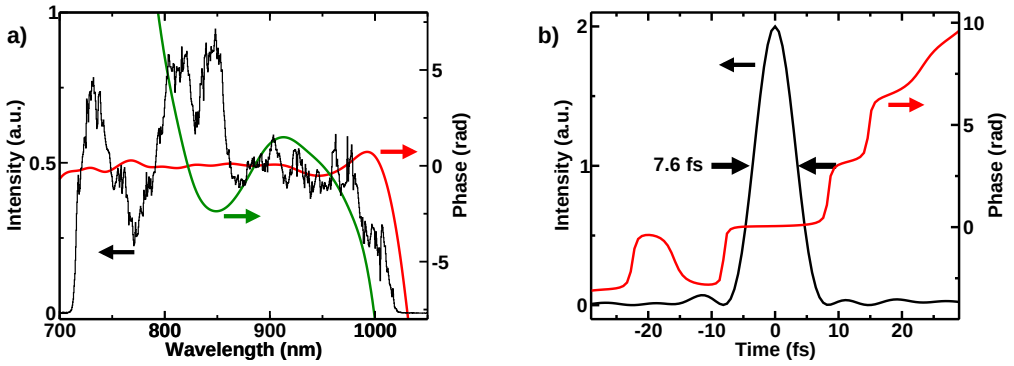

Fig. 4. (a) The spectral intensity (black curve), and spectral phase before (green curve) and after (red curve) adaptive pulse compression with the spatial light modulator. These spectral phase curves have been measured using SPIDER. (b) The reconstructed pulse intensity and phase in the time domain.

3. Spectral phase shaping and few-cycle pulse compression

The stretching and recompression needed for chirped pulse amplification can present serious problems when few-cycle pulses are involved, due to the large bandwidth over which the dispersion needs to be compensated with high accuracy. To date, mJ-level few-cycle pulse sources all employ the output pulses of a relatively narrow-band chirped pulse amplifier, which are spectrally broadened in a nonlinear medium [15, 16, 17]. Such pulses require only a minor amount of chirp compensation that can readily be provided by chirped mirrors. Full chirped pulse amplification and recompression for a broad bandwidth with a large stretching ratio has - to the best of our knowledge - not been demonstrated so far for sub-10-fs pulses, although Takada et al. have reported on a stretcher-compressor system for 8 fs pulses, which they employed in the compression of terawatt-level pulses to 12 fs [18].

The options for broadband stretching and compression are limited. For instance, prism compressors would become impractically large for such broad spectra, even when multiple prism sequences are used. Negative dispersion stretching and subsequent bulk glass compression may be applicable to few-cycle pulses [10], and has the advantage of a high compressor efficiency. However, the extreme power densities of a terawatt-class amplifier can easily lead to self-phase-modulation in the bulk material, or distortion of the wavefront due to glass inhomogeneities when larger beam diameters are used. Instead, we have implemented a grating-based stretcher and compressor system. Although the throughput is typically limited to $\sim$50% (after four grating bounces), such a system can be realized in a much smaller setup with only reflective optics.

We have designed a grating stretcher and compressor combination for 400 nm wide spectra that can compensate dispersion up to third order. This is facilitated by different groove densities (600 l/mm in the stretcher, 1200 l/mm in the compressor), and by putting the compressor grating pair on a rotatable platform, such that the input angle on the gratings can be tuned (thereby varying the ratio between the different dispersion orders) without affecting the overall alignment. The latter is possible due to the small stretching ratio required for NOPCPA, leading to a very compact compressor with a grating separation of only $\sim$20 mm. To counteract higher-order dispersion, a 640-element LCD spatial light modulator (SLM) is incorporated in the Fourier plane of the pulse stretcher, allowing adaptive control over the spectral phase.

The stretcher and BBO crystals together yield a dispersion of 6.3×10^4 fs^2, -9.54×10^4 fs^3 and 1.88×10^5 fs^4 for the second, third and fourth order dispersion, respectively. Throughout the entire setup we have only used gold-coated mirrors, which have a negligible contribution

#72557 - $15.00 USD Received 30 June 2006; revised 18 August 2006; accepted 25 August 2006

to the dispersion. The dispersion of air is not taken into account, as the total beam path from oscillator to compressor output is only 13 meters. The compressor can be tuned to compensate the second and third order dispersion, so that a residual fourth order dispersion of about 4.0×10^4 fs^4 remains. Considering the spectral bandwidth of the pulses and the Nyquist limit of the SLM, we calculate that up to 5.34×10^4 fs^4 can be compensated by adaptive phase-shaping. In practice, the requirements on the SLM are eased by partially canceling the excess higher-order phase deviations through over-compensation of the lower-order phase terms. This is done by aligning the compressor while monitoring the spectral phase in real-time using SPIDER [19] such that the residual phase excursions are well within the range of the SLM across the entire spectrum.

The results of the adaptive pulse compression are shown in Fig. 4(a). Initially, the spectral phase after compression shows deviations ranging from 55 rad at 710 nm to -20 rad at 1020 nm. After adaptive phase shaping with the SLM, the measured residual spectral phase remains within 0.6 rad between 710 and 930 nm, while only above 1000 nm it exceeds 1 rad. The resulting intensity and phase in the time domain are depicted in Fig. 4(b). The FWHM pulse duration is 7.6 fs, which is within 5% of the 7.3 fs Fourier limit. Some minor pre- and postpulses around $\pm$11 fs are observed, which are caused by a combination of the residual spectral phase and the rectangular shape of the spectrum. Due to the 52% compressor efficiency, the pulse energy after compression is reduced to 15.5 mJ. This corresponds to pulses with a duration of only 2.7 optical cycles and a peak intensity of 2 TW.

4. Pulse contrast measurements

An important issue in NOPCPA is the amount of parametric fluorescence that is generated in the various amplifier stages. Especially fluorescence from the first pass (where the gain is highest) can be amplified in subsequent passes to form a significant fraction of the total OPA output, limiting the attainable pulse contrast. In our present amplifier system, we made an initial measurement of the amplified fluorescence by blocking the seed light, in which case 0.3% of the total amplified pulse energy remains. However, as the presence of the seed beam will decrease the gain for the fluorescence, the total integrated fluorescence will be less under normal operating conditions. This difference can be determined by cutting away part of the seed spectrum in the grating stretcher, and monitoring the idler wavelength that corresponds to this "missing" signal spectrum. An increase in the intensity of this particular idler wavelength is then observed when the seed beam is blocked. From these combined measurements, a total integrated fluorescence of 0.2% in the presence of seed light is deduced.

More detailed information on the parametric fluorescence background can be obtained from a high-dynamic-range autocorrelation measurement. However, such a measurement of the pulse contrast is not trivial when compressed few-cycle pulses are involved, due to the large spectral bandwidth and the sensitivity to chirp. A high-dynamic-range pulse contrast measurement usually requires two cascaded second-order processes, such as SHG and subsequent sum frequency generation to obtain the third harmonic. For a reliable measurement, these upconversion processes should induce no spectral modulation or significant pulse stretching, as any such distortions would immediately appear as a reduced pulse contrast. Third harmonic generation is very sensitive to a properly matched pulse duration of the fundamental and second harmonic in the process of sum frequency generation, while the fluorescence background is hardly affected by such a chirp. For this reason, we constructed a high-dynamic-range autocorrelator based on optical parametric amplification [20], which allows for a larger spectral bandwidth than conventional third-order autocorrelation. In this scheme, the second harmonic of the input pulse is used to pump an OPA, seeded by another part of the input pulse. The contrast can then be measured by monitoring the intensity of the produced idler while scanning the pump-seed

#72557 - $15.00 USD Received 30 June 2006; revised 18 August 2006; accepted 25 August 2006

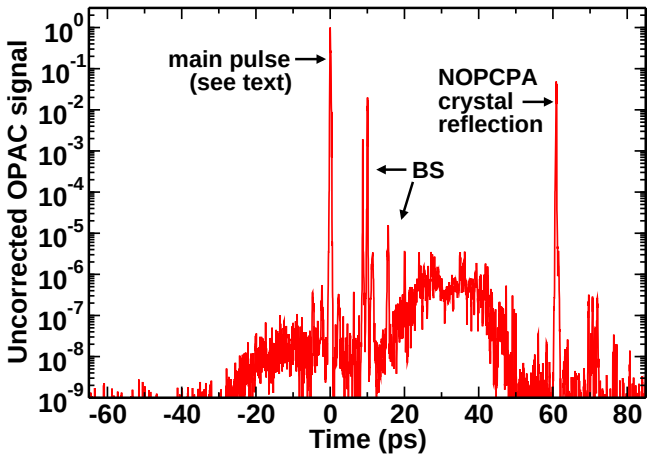

Fig. 5. Uncorrected measurement (raw data) of the pulse contrast using an OPA correlator. A few spurious post-pulses can be seen (BS), caused by beamsplitters in the NOPCPA setup. The peak at 60 ps results from a double internal reflection in the first NOPCPA crystal. The fluorescence background peaks at the 10^{-6} level, but stays below 10^{-7} on the leading edge of the pulse. At times when there is no pump light present, the pulse contrast exceeds the detection limit. The height of the main pulse still needs to be corrected for the effects of pulse broadening in the OPAC: by taking this effect into account, the actual pre-pulse contrast is found to be better than 2×10^{-8}.

delay.

This type of pulse contrast measurement with an OPA correlator (OPAC) is described in detail in [20], although the characterization of few-cycle pulses requires some modifications, as discussed by Tavella et al. [21] for the case of third-harmonic autocorrelation. Firstly, attenuation of the seed pulse in the OPAC is done by taking reflections of wedged fused silica substrates (R$\sim$0.3%) instead of using (dispersive) neutral density filters. Only for the measurement scans with the highest attenuation, one additional thin gray filter (either 12$\times$ or 88$\times$ attenuation) has been used. Secondly, a thin crystal (0.2 mm) is used for SHG to minimize chirp and spectral narrowing. Finally, the noncollinear angle in the 1 mm long OPAC crystal is set at 4° instead of 10° as used in [20] to keep the pulse front tilt small.

A typical pulse contrast measurement is shown in Fig. 5. Aside from the main pulse, several features can be readily identified: first, a fluorescence background is observed between -25 and +50 ps; second, several post-pulses are seen, most notably at 8.6 and 10 ps, which can be traced back to beamsplitters in the NOPCPA setup; third, two pre-pulses at the 10^{-7} level appear at 2.2 ps and 4.4 ps, corresponding to multiple internal reflections of the pump beam inside the 0.2 mm SHG crystal in the OPAC (note that a post-pulse in the pump beam will show up as an artificial pre-pulse in the measurement when scanning the pump-seed time delay); fourth, a significant post-pulse at 60 ps delay arises from a double internal reflection of the signal pulse in the first NOPCPA crystal.

Before attaching any significance to the relative intensities of these features, it should be realized that contrast measurements of few-cycle pulses are easily distorted by various systematic effects. For instance, the SHG used in the OPAC causes spectral narrowing and therefore a longer pulse. In our case, this SHG pulse is estimated to be $\sim$40 fs. The effect of such a pulse duration mismatch on the measured OPAC signal is depicted in Fig. 6. A schematic of a contrast measurement with fundamental seed and SHG pump pulses of equal duration is shown in Fig. 6(a), while in Fig. 6(b) the pump pulse is significantly longer than the seed. Comparing

#72557 - $15.00 USD Received 30 June 2006; revised 18 August 2006; accepted 25 August 2006

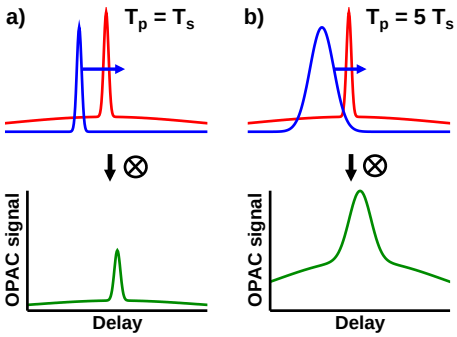

Fig. 6. The influence of a pulse duration mismatch in the OPAC. Pump pulse duration T_p is (a) equal to the seed pulse duration T_s; (b) longer than the seed pulse duration. In both (a) and (b) the red trace represents a short seed pulse on top of a long fluorescence background, while the blue trace represents the pump pulse. A comparison of (a) and (b) reveals that the use of a pump pulse which is longer than the seed pulse leads to a decrease of the measured contrast ratio between the main pulse and the fluorescence (note that all graphs have a linear scale).

these two figures, one can see that a stretched pump pulse not only leads to broader peaks, but also to a decrease of the measured contrast between main pulse and fluorescence background. A quantitative analysis of this effect is performed by calculating convolutions of model pulses with varying pulse duration mismatch. We find that the pulse contrast decreases by a factor approximately equal to the ratio of pump and seed pulse durations, assuming an unchirped seed pulse. A chirp in the seed pulse has negligible effect provided that the seed pulse remains shorter than the pump pulse. Therefore, to correct for the spectral narrowing of the SHG pulse in the present system, the measured pulse contrast from Fig. 5 needs to be increased by an estimated factor of about 5.

The peak at 60 ps also requires careful analysis. This peak can be identified as a double internal reflection (DIR) in the 5.5 mm long NOPCPA crystal, which is amplified by the tail of the pump pulse. Since this pulse is chirped to a duration of 13 ps, its spectral content varies in time and only the longer wavelengths (which are ahead) will be amplified by the tail of the pump pulse. To estimate the spectrum of the DIR pulse after the amplifier, we delayed the seed pulse by 60 ps with respect to the pump. The measured output spectrum has a FWHM of 32 nm centered at 965 nm, which corresponds to a Fourier limit of 43 fs. Because this pulse travels through an additional 11 mm of BBO compared to the main pulse, it will be chirped to about 55 fs when the main pulse is properly compressed. As this pulse is longer than the SHG pump pulse of the OPAC, the contrast of the DIR peak compared to the fluorescence background is realistic, i.e. no correction factor is required in this case. This implies that the present DIR pulse has a peak intensity of less than 1% of the main pulse. However, since it is longer than the main pulse, the total energy content of this DIR pulse is estimated to be about 5%. This DIR pulse energy can be decreased by delaying the seed pulse with respect to the pump, but the present configuration in which the seed pulse timing is set more towards the front of the pump pulse is highly beneficial for the pre-pulse contrast. In Fig. 5, a small pre-pulse might also be expected due to the cross-correlation of the SHG of this DIR pulse with the fundamental of the main peak. However, since the spectrum around 965 nm of the DIR pulse is not phase-matched for frequency doubling in the OPAC SHG crystal, such a pre-pulse is not detected.

Taking the aforementioned correction factor of 5 into account, the observed fluorescence background reaches a maximum value of about 4×10^{-7}, but only after the main pulse. The

#72557 - $15.00 USD Received 30 June 2006; revised 18 August 2006; accepted 25 August 2006

fluorescence level preceding the pulse reaches 2×10^{-8}, and stays below the detection limit of 2×10^{-10} until the onset of the pump pulse at -28 ps. As the shape of the amplified spectrum (see Fig. 2) displays the steep edges that are typical for a saturated NOPCPA system, the corresponding pulse in the time domain has some sidebands that rapidly decay in intensity [22]. Therefore, the measured pre-pulse contrast of 2×10^{-8} will only be reached at times $>$600 fs before the main pulse. Due to the measurement uncertainty and the required correction factor, the accuracy of the present pulse contrast determination is estimated to be about a factor of 2. The integrated fluorescence background from the measurement shown in Fig. 5 is found to be $\sim$0.1% of the main pulse energy, which is in fair agreement with the measured value of 0.2% total integrated fluorescence deduced earlier. The presently achieved pulse contrast constitutes an improvement of more than 3 orders of magnitude over previously published results on the pulse contrast of a short-pulse NOPCPA system [21]. It is interesting to note that even though the measured contrast is comparable to typical Ti:Sapphire multi-pass amplifiers, in an NOPCPA system the fluorescence is only present for the duration of the pump pulse, which is orders of magnitude shorter than the inversion lifetime of Ti:Sapphire. Therefore, the total integrated fluorescence energy can be small in comparison.

The possibility of replica pulses produced by the SLM [23] has also been investigated by repeating the contrast measurement with a large linear phase pattern applied to the pulse shaper. No additional peak structure related to the SLM could be observed within the measurement sensitivity. This can be explained by the large spectral bandwidth of the pulses, leading to a significant "nonlinear spectral dispersion" [23] as the frequency components are not linearly spread across the SLM pixels. Any replica pulse generated by pixelation and phase-wrapping errors of the SLM will therefore be chirped to a duration of several picoseconds, leading to a strong decrease in the replica pulse intensity. In addition, the SLM is used in a double-pass configuration. This means that the phase mask steps are halved compared to single-pass implementations, and also that subtle alignment variations between the two passes through the device induce smoothing of the diffracted spectrum, leading to a decrease in the intensity of possible replica pulses.

5. Conclusions

In conclusion, we have demonstrated the generation of 7.6 fs laser pulses (2.7 optical cycles) with a 2 terawatt peak intensity at 30 Hz repetition rate, based on noncollinear optical parametric chirped pulse amplification. By using an ultra-broadband Ti:Sapphire oscillator as the seed source, the full spectral gain bandwidth of the 532 nm pumped BBO-based NOPCPA could be utilized, leading to the direct amplification of 310 nm wide spectra to 30 mJ pulse energy. Stretching by a factor of $\sim2\times10^3$ and near-Fourier-limited recompression of these ultra-broadband spectra is performed using a grating-based pulse stretcher with an LCD phase-shaper, and a grating-pair pulse compressor. Important system characteristics such as beam profile, intensity stability and pulse contrast have been investigated, and are found to be of good quality. The pre-pulse contrast reaches 2×10^{-8} on short timescales, and exceeds the 2×10^{-10} detection limit of our contrast measurement setup on timescales $>$28 ps.

Due to the compactness of the setup, the absence of thermal effects, and the existing Nd:YAG laser technology, scaling of the intensity by orders of magnitude looks promising, which might allow the generation of sub-3-cycle pulses with an intensity approaching the 100 TW level.

Acknowledgments

This project is financially supported by the Foundation for Fundamental Research on Matter (FOM), the Netherlands Organization for Scientific Research (NWO), and the EU Integrated Initiative FP6 program Laserlab-Europe. These contributions are gratefully acknowledged.